ACS APPLIED MATERIALS & INTERFACES

Research Article

Cite This: ACS Appl. Mater. Interfaces 2019, 11, 33336−33346

www.acsami.org

All-Textile Electronic Skin Enabled by Highly Elastic Spacer Fabric and Conductive Fibers

Ronghui Wu,[†,‡,§] Liyun Ma,[†,‡] Aniruddha Patil,[†] Chen Hou,[†] Shuihong Zhu,[†] Xuwei Fan,[∥] Hezhi Lin,[∥] Weidong Yu,[*,†,‡] Wenxi Guo,[*,†] and Xiang Yang Liu[*,§,†]

[†]Research Institution for Biomimetics and Soft Matter, Fujian Provincial Key Laboratory for Soft Functional Materials Research, College of Physical Science and Technology, Jiujiang Research Institute, Xiamen University, Xiamen 361005, China

[‡]Key Laboratory of Textile Science & Technology, Ministry of Education, College of Textiles, Donghua University, Shanghai 201620, China

[§]Department of Physics, Faculty of Science, National University of Singapore, Singapore 117542, Singapore

[∥]Department of Information and Communication Engineering, Xiamen University, Xiamen 361005, China

Supporting Information

ABSTRACT: Electronic fabrics that combine traditional fabric with intelligent functionalities have attracted increasing attention. Here an all-fabric pressure sensor with a wireless battery-free monitoring system was successfully fabricated, where a 3D penetrated fabric sandwiched between two highly conductive fabric electrodes acts as a dielectric layer. Thanks to the good elastic recovery of the spacer fabric, the capacitance pressure sensor exhibits a high sensitivity of 0.283 KPa^{-1} with a fast response time and good cycling stability (≥20 000). Water-soluble poly(vinyl alcohol) template-assisted silver nanofibers were constructed on the high-roughness fabric surface to achieve high conductivity (0.33 Ω/sq), remarkable mechanical robustness, and good biocompatibility with human skin. In addition, the coplanar fabric sensor arrays were successfully designed and fabricated to spatially map resolved pressure information. More importantly, the gas-permeable fabrics can be stuck on the skin for wireless real-time pressure detection through a fiber inductor coil with a resonant frequency shift sensitivity of 6.8 MHz/kPa. Our all-fabric sensor is more suitable for textile technology compared with traditional pressure sensors and exhibited wide potential applications in the field of intelligent fabric for electronic skin.

KEYWORDS: *conductive fabric, electrostatic spinning, 3d penetrated fabric, pressure sensor, wireless passive sensor*

1. INTRODUCTION

With the development of advanced flexible and wearable devices, electronic textiles (E-textiles) that integrate various electronics such as sensors,[1,2] energy-harvesting devices,[3−5] and antennas[6,7] into fabrics have attracted considerable interest due to their great potential applications in the smart, living, health care, and medication fields in combination with big data and artificial intelligence (AI). As an essential component of E-textiles, wearable pressure or strain sensors, which can respond to environmental stimuli, have been well studied in recent years.[8]

In general, there are three types of sensing mechanisms for E-textile-based sensors, resistive,[1,9−11] capacitive,[2,12,13] and self-powering.[14−16] For capacitive pressure sensors, the conductive fabrics usually act as electrodes, and the rubber-like materials sandwiched between two conductive fabric layers,[12,17] such as polydimethylsiloxane (PDMS),[1] polyurethane (PU),[18] Eco-flex,[19−21] and latex,[22] usually act as dielectric layers. Despite the great efforts that have been devoted to develop fabric pressure sensors, there are some problems that still remain to be solved. First of all, it is difficult to obtain highly conductive textiles because of the wavy structure of the fabric surface, not to mention the stretchable conductive fabric electrodes.[23,24] Although tremendous efforts have been made to improve the conductivity of fabrics by coating conductive metal (or carbon) films, satisfactory or comparable performance to that of the flat film substrate has still not been achieved. Moreover, the obtained fabric conductivity was accompanied by the sacrifice of the fabric surface morphology and style due to the coating or composite spinning.[23,25] Second, rubber-like dielectric layers including PDMS, PU, and Eco-flex are heavy and airtight, which is not suitable for long-term wear. An ideal solution for preparing a rubber-free dielectric layer is to construct a high-elastic-recovery penetrated fabric directly sandwiched between sensor electrodes by traditional textile technology. The 3D warp-

Received: June 21, 2019
Accepted: August 19, 2019
Published: August 19, 2019

DOI: 10.1021/acsami.9b10928
ACS Appl. Mater. Interfaces 2019, 11, 33336−33346

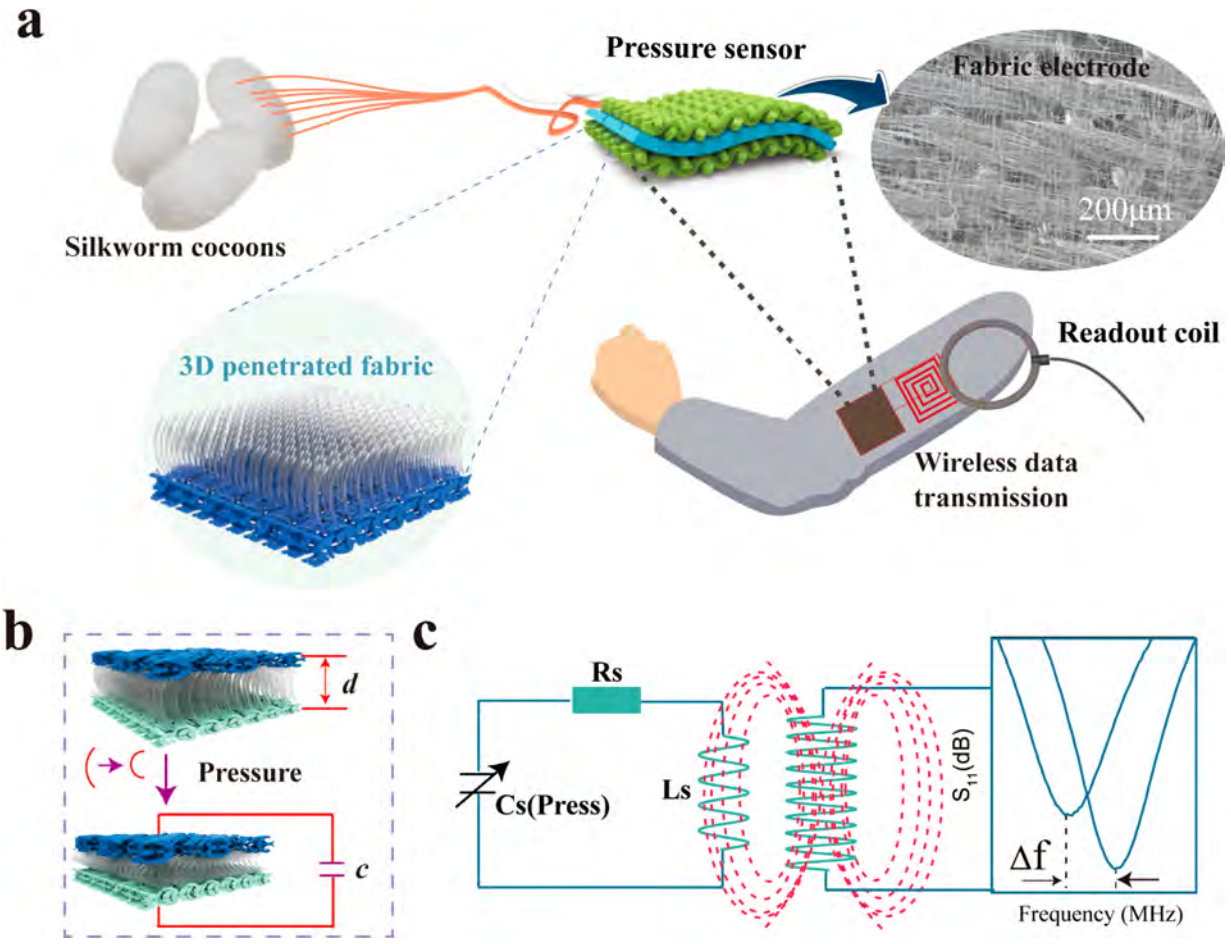

Figure 1. Schematic of the strategy for the fabrication of the LC wireless all-textile pressure sensor. (a) Schematic of the LC monitoring pressure sensor, which combines a flexible all-fabric pressing sensor containing conductive fabric electrodes and 3D penetrated fabric with a LC wireless sensing system based on the fiber inductor coil. (b) Schematic of the 3D penetrated fabric as dielectric layer for the capacitance sensor during changing under pressure. (c) Schematic of the wireless monitoring system for the capacitance sensor.

knitted spacer fabric that consists of two independent fabrics and a layer of spacer yarns as the connection in between bears a very good size stability of the surface structure and excellent mechanical properties, which makes it a promising material for flexible electronics.[26−28] Third, for lightweight wearable and mobile electronic devices, we must get rid of the traditional bulky detection and power supply devices,[5] and we realize that the wireless transmission/control of signals is still an issue. The intrinsic wireless passive inductor−capacitor (LC) resonance method is a good candidate in harsh measurement environments because of its lower operating frequency and near-field coupling distance;[29] therefore, it has been developed in various situations.[30] Recently, textile-based wireless sensors with a resonant circuit have attracted many researchers' interests.[31] However, an intrinsic all-textile wireless passive pressure sensor with fiber inductance and a fibrous sensing capacitor without a polymer film and adhesive is still challenging because of the difficulty in designing the inductance and other electronic components on fabric. Hence, developing an all-fabric (rubber-like material-free) wireless monitoring pressure sensor that is flexible, stretchable, wearable, and breathable with wireless monitoring ability is challenging and urgently needed.

To address the aforementioned problems, three strategies were adopted in this work. First, water-soluble poly(vinyl alcohol) (PVA) template-assisted silver nanofibers (Ag NFs) with high conductance and mechanical flexibility were transferred on the fabrics surface to serve as sensor electrodes. The obtained conductive fabrics showed a sheet resistance of 0.33 Ω/sq without the sacrifice of the original fabric pattern and style. Second, the highly elastic 3D penetrated fabric, which has a good size stability of the surface structure and excellent mechanical properties, was utilized as the capacitance dielectric layer. Third, the wearable fiber inductor coil was embedded into fabrics for signal transmission. A textile-based LC circuit wireless and battery-free sensing system was established using a well-developed radio frequency coupling method. Furthermore, large-area sensor arrays were successfully fabricated on one textile substrate to spatially map tactile stimuli and directly incorporated into a glove for pressure mapping. The ingenious structure of fabric based on a flexible and wearable sensor with good properties has wide potential applications and has provided a prospect in the field of intelligent fabric for electronic skin and the acquisition of human motions and health data.

2. RESULTS AND DISCUSSION

The wireless pressure-sensing device for wearable E-textiles should be versatile for fashionable and comfortable designs. Figure 1a illustrates the schematic of the LC monitoring wearable pressure sensor, which combines a flexible all-fabric pressing sensor containing a conductive fabric electrode and

DOI: 10.1021/acsami.9b10928
ACS Appl. Mater. Interfaces 2019, 11, 33336−33346

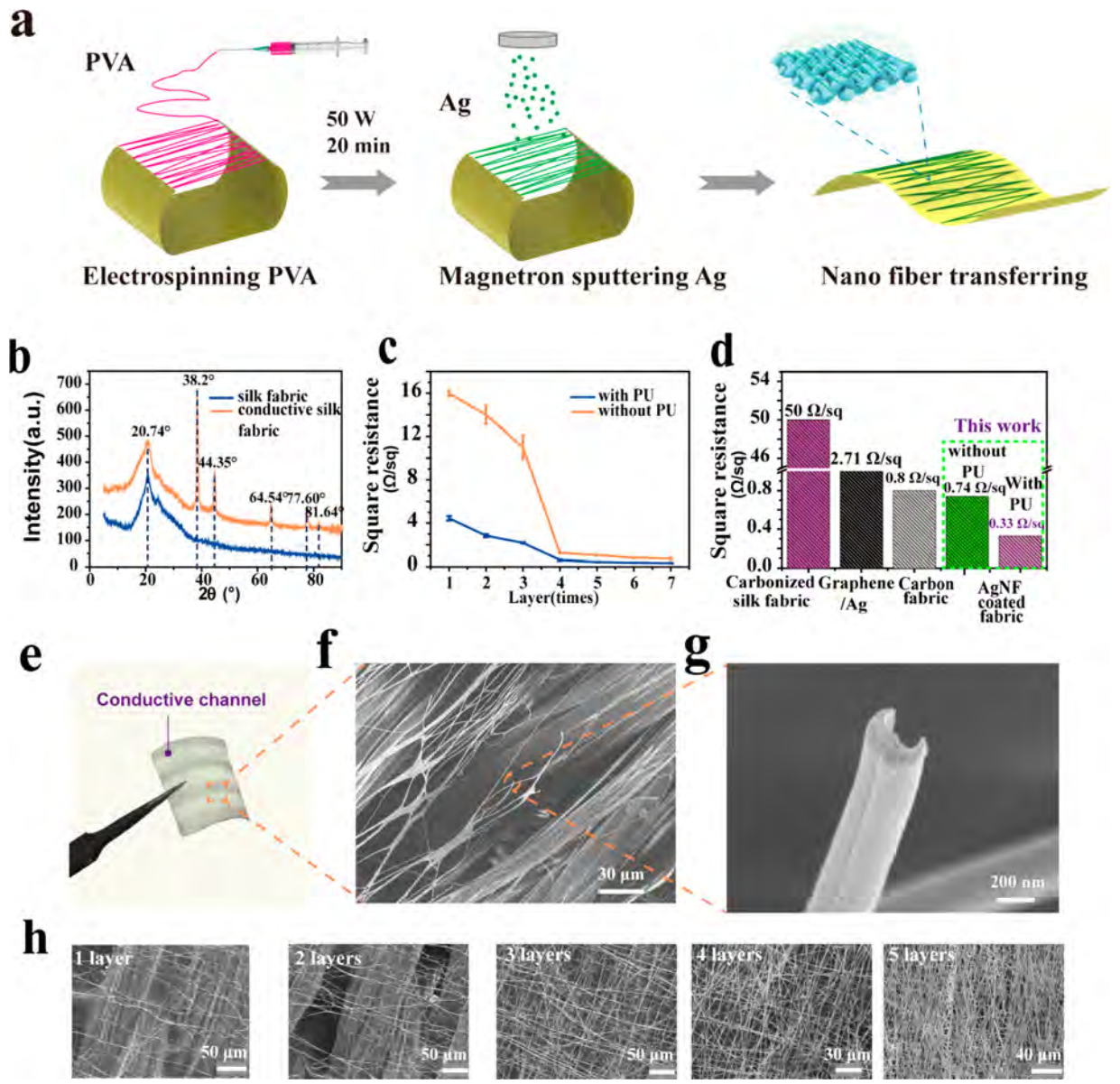

Figure 2. Preparation and characterization of the color-reserved highly conductive fabric. (a) Preparation process of conductive fabric electrodes: fabricating PVA NFs by electrospinning and then magnetron sputtering of Ag on the fiber surface, followed by transferring the conductive NFs on the fabric surface. (b) XRD spectra of the original and conductive silk substrate fabric. (c) Square resistance of the color-reserved conductive fabric as the number of transferred fiber network layers increases from one to seven, with and without polyurethane (PU) as the bonding layer. (d) Comparison of electric properties between as-prepared fabric and previously reported conductive fabrics in refs 19 and 32. (e) Surface morphology of the conductive fabric, with the fiber network bonded on the surface (f). (g) Groove-like morphology of electrospinning fibers after magnetron sputtering and PVA template removal. (h) Surface topography of the conductive fabric surface as the number of transferred layers increases.

3D penetrated fabric with an LC wireless sensing system based on the fiber inductor coil. In this configuration, high-density Ag NF networks were constructed on the silk fabrics to improve the conductivity and flexibility, and highly elastic 3D penetrated fabric was sandwiched between the electrodes to replace the rubber dielectric layer. When the pressure was applied, the space (d) between the electrodes changed (Figure 1b), thereby increasing the capacitance of the textile sensors; this then lead to the frequency shift of the LC wireless testing system (Figure 1c).

As shown in Figure 2a, Ag NFs were constructed on the fabrics by electrostatic spinning and subsequent magnetron sputtering methods, which are compatible with traditional textile technology. In detail, the conductive NFs were first obtained by magnetron sputtering Ag films on an electrospinning PVA NF template surface. By transferring the different amounts of NFs onto the fabric surface and removing the PVA fiber membrane by deionized water, groove-shaped Ag-NF-coated conductive fabrics (Figure 2f,g) with different appearances could be obtained (Figure 2h). The X-ray diffraction (XRD) spectra of the PVA fiber with and without the Ag coating are shown in Figure 2b. The diffraction peaks located at 38.2, 44.35, 64.54, and 77.6° can be readily indexed to (111), (200), (220), and (311) of pure quasi-amorphous Ag, respectively. The diffraction peak located at 20.74° is a characteristic peak of plain silk fabric, and a negligible change was observed before and after sputtering, indicating that the structure of the silk fabric remained unchanged. The XRD

DOI: 10.1021/acsami.9b10928
ACS Appl. Mater. Interfaces 2019, 11, 33336−33346

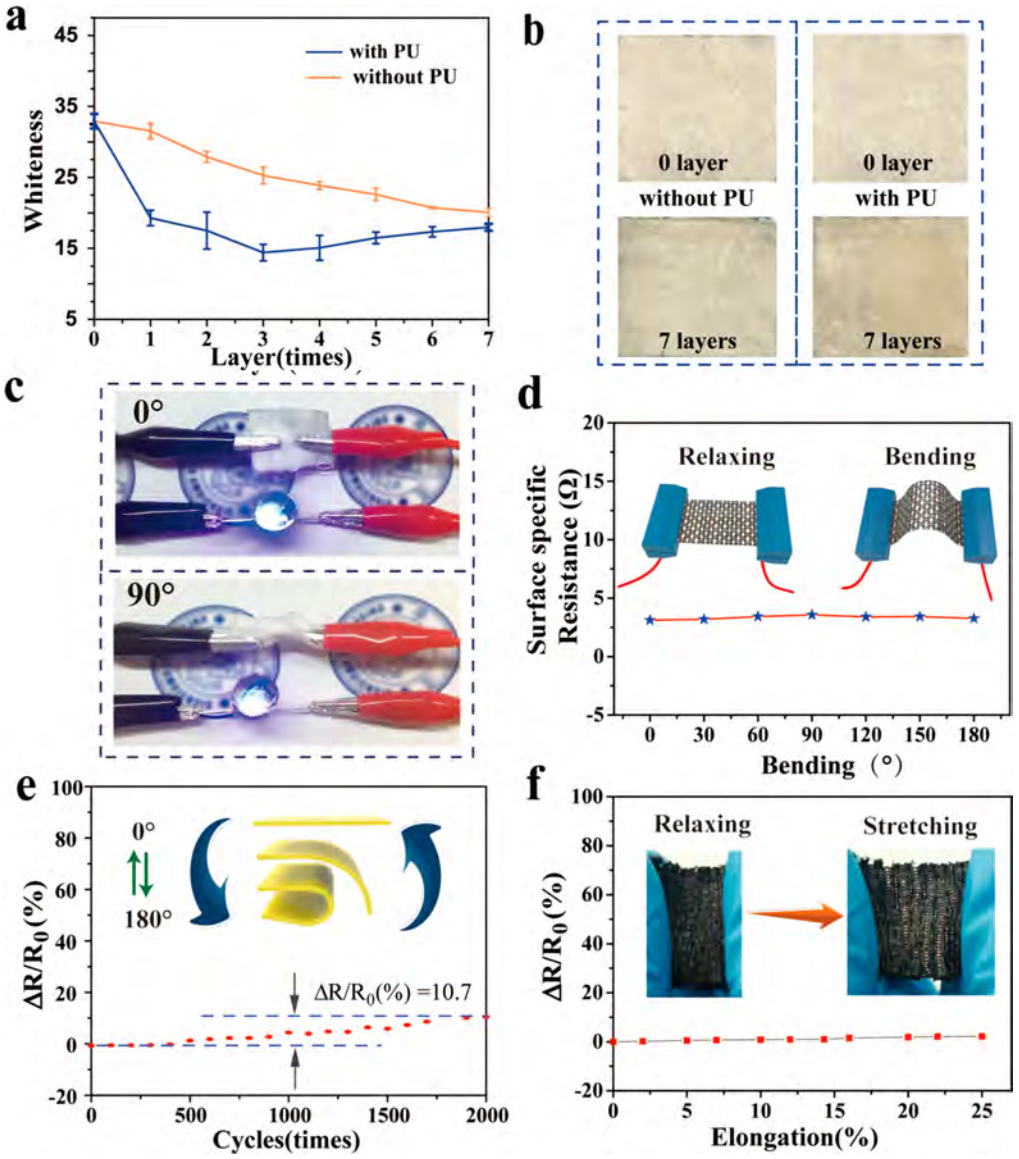

Figure 3. Electrical performance of the highly electric conductive fabric. (a) Whiteness variation of the color-reserved conductive fabric as the number of transferred fiber network layers increases from one to seven, with and without transparent PU as the bonding layer. (b) Images of the color variance of the fabric before and after coating the conductive layers. (c) Photograph of the conductive fabric lighting a bulb as a segment of the circuit when suffering from twisting. (d) Relationship between the specific surface resistance[33] variation and the bending angles of the conductive fabric. (e) Reproducibility of the conductive fabric after bending from 0 to 180° 2000 times. (f) Resistance variation when a conductive rib-knitted fabric was stretched from 0 to 25%.

spectra show that the Ag films were attached on the surface of the silk fabrics. The scanning electron microscopy (SEM) image in Figures 1a and 2e shows that the PVA NFs were on the surface of the fabric. The length of the ultralong NFs can reach several centimeters, which can significantly decrease the number of wire−wire junctions and ultimately enhance the conductivity and mechanical flexibility. The sheet resistance would decrease from 16 to 0.74 Ω/sq by increasing the NFs from one to seven layers on the fabric substrate, as shown in Figure 2c. It is worth mentioning that the sheet resistance can be further decreased to 0.33 Ω/sq by using a transparent PU layer, which is benefit for improving the contact between the silk fabric and NFs. Figure 2d shows the comparison among several typical conductive fabrics. The fabric in our work exhibits the best electric conductivity compared with the previously reported carbon fiber cloth, carbon paper, carbonized fabric, and conductive fabric.[9,23,24]

According to our previous work,[34,35] the film made of Ag NFs was transparent. In this way, it is beneficial for the silk fabric to maintain its original color when the NFs are transferred to its surface, as can be seen in Figure 3b and Figure S1. The whiteness of the fabric decreased only 1.4 units from 32.93 to 31.53 when one layer was transferred (Figure 3a). After coating for seven layers, the whiteness decreased from 32.9 to 20.06. The transparent PU has a slight effect on the fabric surface morphology, as the whiteness decreased to 18.6. Figure 3e and Video S1 show that the electric conductivity of the fabric decreased only 10.7% after bending 2000 times, indicating that the conductive fabric has good flexibility and durability. Further tests, as shown in Figure 3c,d, demonstrated that the conductive fabrics can endure bending

DOI: 10.1021/acsami.9b10928
ACS Appl. Mater. Interfaces 2019, 11, 33336−33346

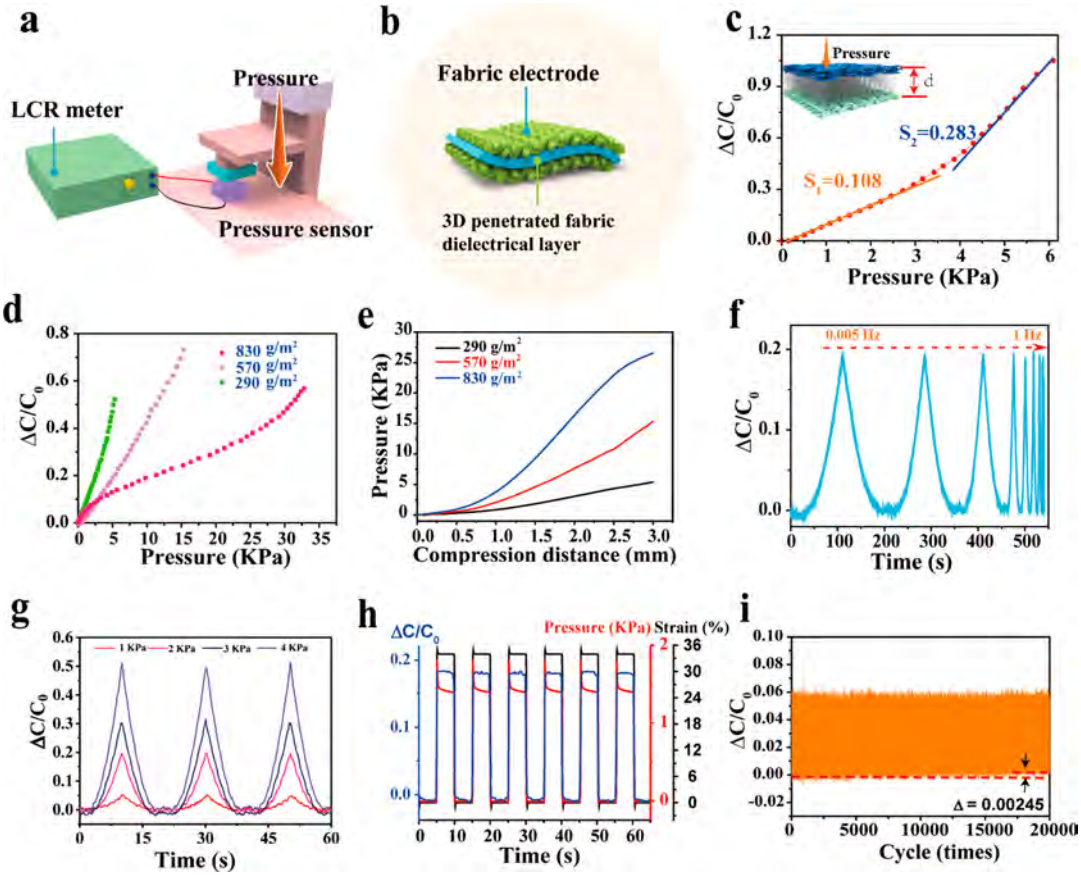

Figure 4. Structure and performance of the all-fabric capacitance pressure sensor. (a) Testing system for the fabric-based pressure sensor. (b) Schematic of the capacitance pressure sensor that consists of a 3D penetrated fabric dielectric layer with conductive fabric electrodes. (c) Relationship between the variation of capacitance and the applied pressure. (d) Performance of the pressure sensor with different weights per square meter of 290, 570, and 830 g/m^2. (e) Compression distance−pressure curves for three fabrics with different parameters. (f) Response of the pressure sensor at different mechanical frequencies of 0.005 to 1 Hz. (g) Capacitance variation when applying different pressures of 1, 2, 3, and 4 KPa on the pressure sensor three times. (h) Capacitance, strain, and pressure variation when applying a load on the sensor, holding, and releasing for 5 s. (i) Reproducibility of the sensor under a pressure of 0.5 KPa for 20 000 cycles of consecutive linear loading−unloading with a pressure frequency of 1 Hz.

and twisting at different angles, which is significant for wearable applications.

Taking advantage of this facile preparation method, conductive fabric of different structures and patterns can be obtained, as the PVA NF template-assisted Ag NF network can be transferred to prestretched fabric stably and easily, as shown in Figure S1. Specifically, the stretchable conductive knitted fabric with a rib-stitch structure was fabricated by transferring Ag NFs to the prestretched knitted fabric, as shown in Figure 3f, and no obvious degradation in electrical conductivity was observed in the strain ranges from 0 to 25%, which enables the electrodes to be used in stretchable and wearable electronics. The superior tensile property can be attributed to the Ag NFs being laminated along the fabric grain, and thus they will not break during the straightening of the ribbed fabric. Moreover, different patterned electricity-conductive fabrics can be prepared by a mask-assisted method. As shown in Figure S2, a fabric electrode for a four-channel pressure sensor (Figure 2e) was fabricated under the mask with adhesive tape by laser cutting. Thus the simplicity of this preparation method and the high electrical conductivity of the Ag-NF-coated fabric make it a good candidate for wearable electronic devices.

By combining the flexible fabric electrodes with an elastic spacer fabric dielectric layer, a fabric-based pressure sensor was fabricated, as illustrated in Figure 4b. The capacitance of the fabric-based pressure sensor can be effectively changed by the incremental load-induced thickness change of the polyester monofilament spacer yarn as well as a regular change in the dielectric constant, ε. When the spacer fabric is under pressure, the spacer yarn is extruded to bend from the stretching state, and it returns to the natural state when the pressure is released. For the spacer-fabric-based capacitance-type pressure sensor, the capacitance of the sensor (C_{sensor}) can be described by the following parameters: electrode area (S), dielectric thickness (d), constant k, and relative permittivity of the dielectric (ε_e). Equation 1 describes the change in capacitance due to variations in the dielectric layer thickness

$$C_{sensor} = \frac{\varepsilon_e S}{4\pi k d} \quad (1)$$

As shown in Figure 1b, when a pressure was applied to the sensor, the dielectric thickness between the two electrodes would decrease. In addition to the dielectric thickness, d, change, the permittivity variation of the dielectric under pressure loading also resulted in a change in capacitance. The dielectric permittivity (ε_e) of the spacer fabric is shown in eq 2

$$\varepsilon_e = \%V_{air}\cdot\varepsilon_{air} + \%V_{PET}\cdot\varepsilon_{PET} \quad (2)$$

DOI: 10.1021/acsami.9b10928
ACS Appl. Mater. Interfaces 2019, 11, 33336−33346

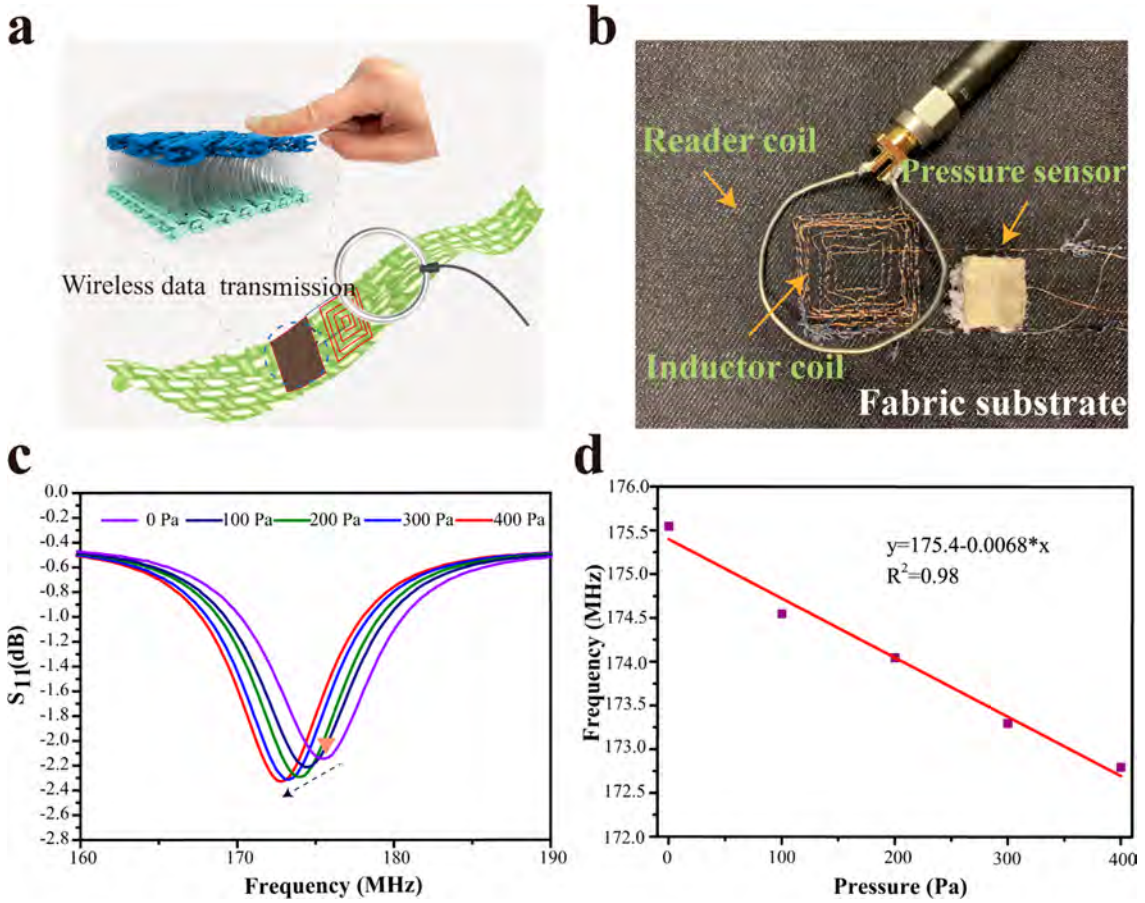

Figure 5. LC wireless passive sensing for the all-textile sensor under pressure. (a) Schematic of the wireless monitoring system for the fabric-based capacitance sensor. (b) Optical image of the capacitance fabric sensor with a fiber inductor coil for LC wireless monitoring. (c) Simulated S_{11} return loss for the LC testing system under pressure from 0 to 400 Pa. (d) Resonance frequency of the fiber LC circuit as a function of pressure.

where ε_{air} = 1 and ε_{PET} = 3.3 and $\%V_{air}$ and $\%V_{PET}$ represent the percentage of air and PET in the volume of the entire dielectric layer. Because the volume of the air gaps will reduce under pressure loading, ε_e will increase overall; therefore, the capacitance increases. The decrease in dielectric thickness (d) and increase in permittivity (ε_e) under pressure together contribute to a high sensitivity of the textile capacitance sensor. The measurement system is illustrated in Figure 4a. The sensitivity (S) of pressure sensor can be defined as $S = \Delta C/C_0/\Delta P$, where ΔC and C_0 represent the change in capacitance and baseline capacitance, respectively, and ΔP represents the change in applied pressure. As shown in Figure 4c, the flexible pressure sensor shows a high sensitivity of 0.108 KPa^{-1} under pressure from 0 to 2.5 KPa and a sensitivity of 0.283 KPa^{-1} under pressure from 4.5 to 6 KPa.

Several kinds of weft-knitted fabrics with different parameters were tested for the pressure sensor by using a polyester monofilament as a spacer yarn and low-stretch polyester filament as a face yarn. As shown in Figure 4d, three kinds of spacer fabrics with different weights per square meter of 290, 570, and 830 g/m^2 were tested. Because the 3D penetrated fabrics were composed of air and the polyester (PET) fibers, we observe a correlation between the weight per square and the sensor performance, as lower weight spacer fibers lead to the same deformation under less applied pressure. It is obvious from Figure 4d that the sensitivity of the fabric sensor increases whereas the detection range decreases when the weight per square meter of the space yarn decreases from 830 to 290 g/m^2. This is because with the spacer fiber density increasing, the compressive modulus of the fabric increases, which is further proved by compression−reply tests, as shown in Figure 4e. In real applications, a sensor with a controllable sensitivity and working range is desirable. Attributed to the controllable working range of our fabric pressure sensors, they can not only monitor the slight movement but also be used to detect large-scale human body movement.

Attributed to the high elastic recovery performance of the spacer fabric dielectric layer, the pressure sensor has a quick and stable response under different mechanical frequencies and amplitudes. As shown in Figure 4f, the pressure sensor has a stable response under a wide mechanical frequency range from 0.005 to 1 Hz. Figure 4g shows the capacitance response when applying and releasing different pressures of 1, 2, 3, and 4 KPa on the sensor three times. The quick and stable reply under different certain forces shows that the pressure sensor has stable and continuous responses for the various loadings. Figure 4h provides the instant capacitance and compression strain response against the quick applied forces, showing that the pressure sensor has an immediate response to external loads. It is worth mentioning that the electric fabric sensor also has a sensitive response to the torsion, as shown in Figure S3. When the pressure sensor is under torsion, the capacitance signal gradually increases with the spiral angle increasing from 10 to 40°. As shown in Figure 4i, the output signals of the pressure sensor composed of conductive fabric electrodes and

DOI: 10.1021/acsami.9b10928
ACS Appl. Mater. Interfaces 2019, 11, 33336−33346

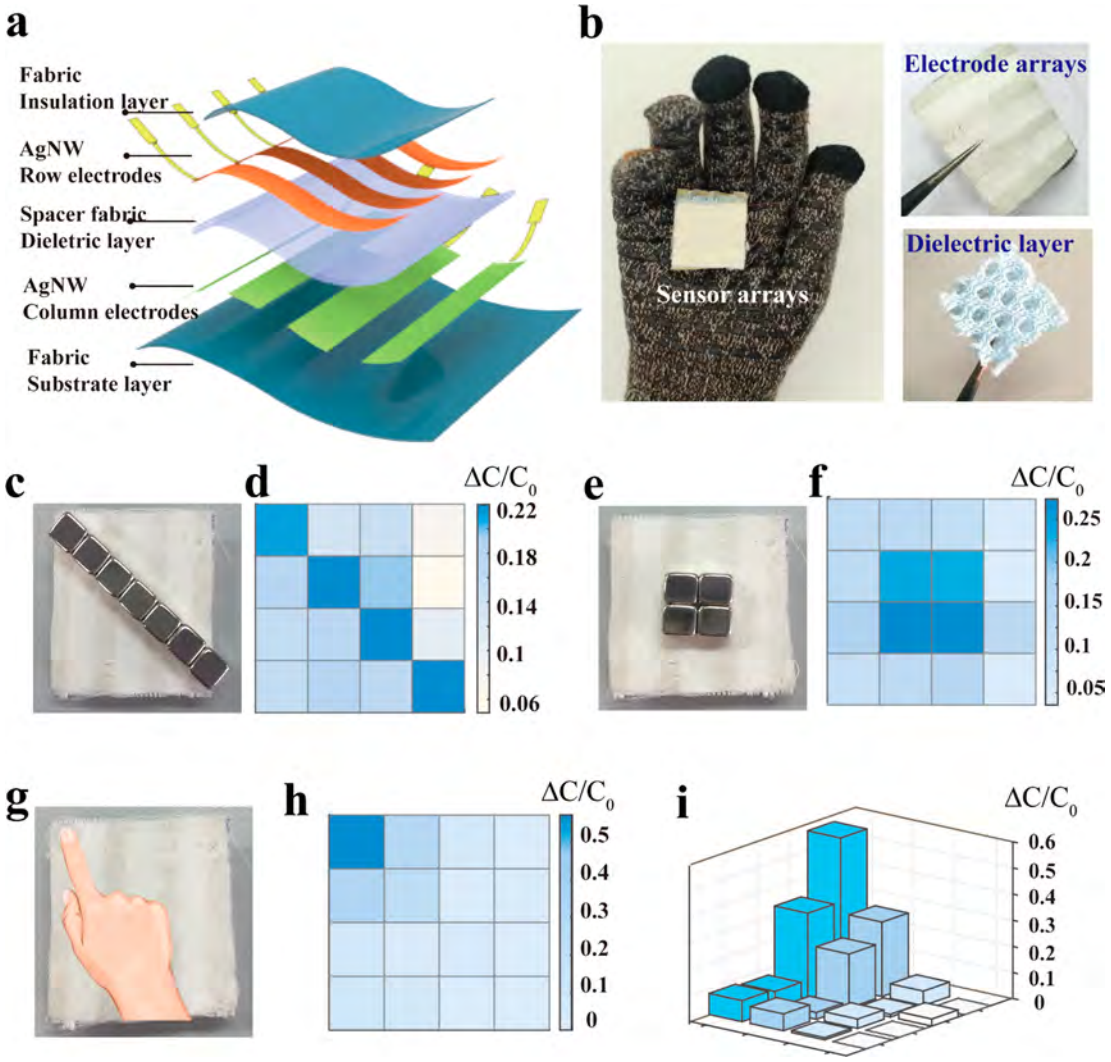

Figure 6. Pressure mapping based on the coplanar all-textile pressure sensor arrays. (a) Schematic description of a textile sensor array with 4 × 4 pixels. (b) Photographs of the sensor arrays, electrode arrays, and spacer fabric dielectric layer. (c,e) Photographs of the sensor array pressed by a slash and a square-shaped weight and (d,f) corresponding mapping of the pressure distribution. (g) Schematic description of the pressure sensor when a finger was pressing on the sensor of the 16 pixels and the corresponding capacitance signals (h) and 3D output signals (i).

a dielectric layer of spaced fabric were stably maintained with a capacitance loss of only 0.002, even after 20 000 intensive cycles, indicating that the textile-based pressure sensor was highly reproducible.

A wearable LC wireless monitoring system was developed for the textile capacitance pressure sensor, as shown in Figure 5a. The wireless circuit consists of an LC resonator circuit, wherein the capacitive sensor is connected in series to a fiber inductor coil, which is sewn in the cotton fabric substrate, as shown in Figure 5b. The change in capacitance results in a frequency shift of the LC resonator, as resonance frequency can be calculated by $f = 1/2\pi\sqrt{LC}$. This shift is wirelessly monitored through the inductive coupling with an external reader coil, and the input transmission coefficient S_{11} is measured on the ports (Figure 1c). The applied pressure has an effect on the capacitance and thus on the resonance frequency values of the resonance circuit. Figure 5c shows that with the pressure increasing from 0 to 400 Pa, the resonance frequency values decrease, in which case the frequency shift of the pressure sensor is 2.8 MHz under a pressure of 400 Pa with a sensitivity of 6.8 MHz/kPa (Figure 5d).

To test the feasibility of tactile sensing for smart textiles, the fabric sensors were designed into a textile sensing array to spatially map pressure information. Unlike the resistance type of multichannel pressure sensor, which requires each sensor unit to be thoroughly separated, and thus complicated electrode arrays were required,[36,37] the capacitance sensor array in this work was of a sandwich structure that combined the fabric planar circuit with a coplanar dielectric layer (Figure 6b), which will simplify the preparation and device design to a large extent. Figure 6a schematically describes the 4-by-4-pixel sensing arrays, with mask-aided patterned conductive silk-based fabric as the bottom and top electrodes and 3D penetrated spaced fabric as the middle dielectric layer material (Figure S4). When a certain weight and pattern fabric was placed on the pressure array, the electrical signals of the pressure sensor arrays were monitored. As shown in Figure 6d,f, the output electrical signals from the pressure sensors clearly demonstrate the loading of the objects (Figure 6c,e). Moreover, human touch during pressure can be monitored by the textile pressure-sensing arrays. Figure 6g,h shows the optical image and signal output and pressure distribution

DOI: 10.1021/acsami.9b10928
ACS Appl. Mater. Interfaces 2019, 11, 33336−33346

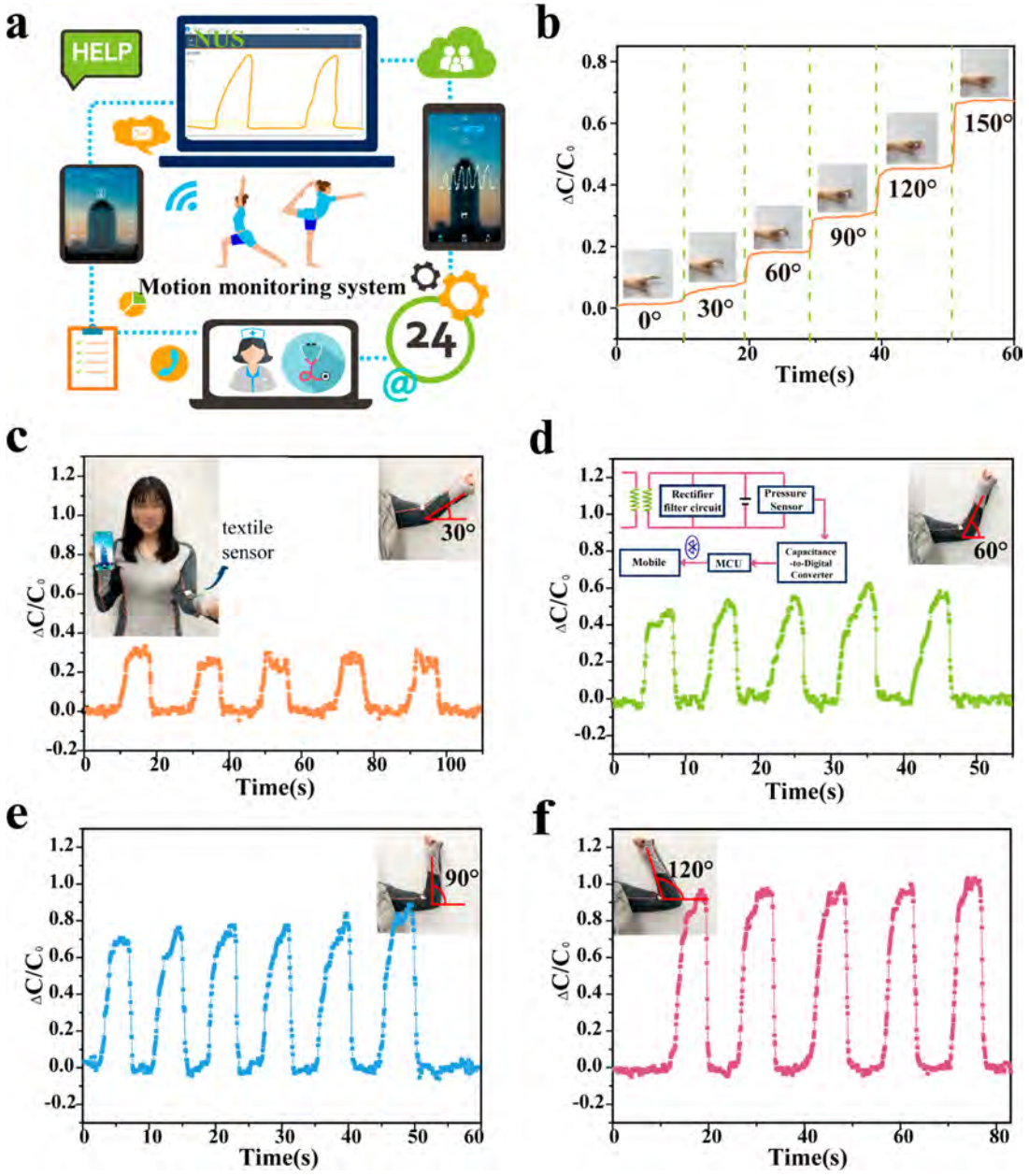

Figure 7. Real-time detection of the human motion using the all-textile pressure sensor. (a) Image and schematic illustrations of the whole system for a motion-monitoring intelligent garment, in which data could be remotely monitored by a mobile application (APP). (b) Optical images and corresponding capacitance variation of a wearable sensor attached on the skin of a bent finger at different angles. The left picture inside panel c is the optical image of a wearable intelligent garment, which imbedded the wearable pressure sensor at the position of the elbow joint. (c–f) Optical images and capacitance variation when the volunteer who wears the intelligent garment bends her elbow joint for (c) 30°, (d) 60°, (e) 90°, and (f) 120°. The diagram inside panel d is the schematic for the capacitance signal detection and transmission.

(Figure 6i) when a certain pressure is applied on the corner of the coplanar sensors. The above results clearly manifested the ability of the conductive silk-based 3D textile pressure sensor and indicated that it has high potential for applications in the human–machine interface and in human activity detection.

Because of the high sensitivity and flexibility and large detection range of the all-textile pressure sensor, it can be embedded into garments to detect human motion like coughing, arm bending, and finger gestures. Besides the LC wireless monitoring system, capacitance signals can be transmitted to mobile terminals (Figure S5) or uploaded to cloud servers (Figure S6) through bluetooth wireless transmission technology for real-time monitoring, as shown in Figure 7a. Figure 7b shows the optical images and corresponding capacitance variation signals of a wearable sensor attached on the skin of a bent finger at different angles. Once the finger is bent, the capacitance of the all-fabric pressure sensor will increase because the sensor squeezing during bending leads to pressure on the sensor. More interesting, by sewing the fabric pressure sensor on the sleeve of the sporting garment, the capacitance change and corresponding precise bending angle can be detected, as can be seen in Figure 7c–f and Video S2. The inset of Figure 7d illustrates the schematic diagram for the capacitance signal detection and transmission. In addition, the textile sensor was attached onto the skin of the neck to noninvasively monitor

DOI: 10.1021/acsami.9b10928
ACS Appl. Mater. Interfaces 2019, 11, 33336–33346

the pressure difference of the muscle movement during human coughing, and the fabric pressure sensor exhibited obvious and consistent signals during coughing five times, as shown in Figure S7.

3. CONCLUSIONS

In this work, an all-fabric wireless pressure sensor based on the textile circuit was fabricated. For the fabric electrode, a highly conductive fabric with a square resistance of 0.33 Ω/sq was obtained by transferring water-soluble PVA nanofiber template-assisted Ag NFs on the fabric surface without the sacrifice of original fabric pattern and style. The pressure sensor with a 3D penetrated spaced fabric dielectric layer exhibited high sensitivity of 0.283 KPa^{-1}, a quick response, and good stability(≥20 000 cycles). The frequency shift of the textile LC circuit for the capacitance pressure sensor has a high sensitivity. In addition, the coplanar 4-by-4-pixel fabric sensing arrays based on patterned silk fabric electrodes and 3D penetrated fabric were designed to display the pattern of the object. The ingenious structure of fabric based on a flexible and wearable sensor with good properties has provided a prospect in the field of intelligent fabric to acquire human motions with wireless transition and detection.

4. EXPERIMENTAL SECTION

Preparation of Conductive Fabric. The silk fabric was washed in a solution of acetone for 30 min, followed by alcohol washing for 10 min and drying in the oven at 60 °C. This process was repeated three times. The nanowire network with high continuity and conductivity was obtained by two steps as follows: The free-standing PVA nanofibers were fabricated on an aluminum frame by electrospinning with a positive voltage of 15 kV and a negative voltage of 1.5 kV. Second, the Ag thin layer was sputtered on the PVA networks by magnetron sputtering at room temperature, with argon pressure of 0.4 Pa and a sputtering power of 50 W for 20 min. The silk fabric was first coated with a layer of PU. Then, the metallized fibers were transferred to the pretreated silk fabric, and the Ag nanotroughs were derived after removing the PVA nanofibers using deionized water. For the stretchable conductive ribbed fabric, the fabric substrate was first stretched to 25%, at which state metallized fibers were transferred onto the surface. After the PVA nanofibers were removed, the ribbed fabric was released to the original state. These raw fabrics were provided by Guangzhou Xianxiangyu Textile Limited Company.

Preparation of the Flexible Pressure Sensor. An enameled Cu wire was attached on the side of silk fabric by a conductive silver paste (Dupont 4929N), with a conductive resin stabilizing the linkage segment. A conductive fabric with a Cu electrode was then encapsulated by PU. Spacer fabrics with different fabric weights per square meter of 290, 570, and 830 g/m^2 at size 2 × 2 cm^2 were used for the dielectric layer of the pressure sensor. The prepared encapsulated conductive silk fabric was attached on both sides of the spacer fabric with a double-sided fusible interlining by the hot-pressing method.

Preparation of the LC Wireless Pressure-Sensing System. Enameled copper wire was stitched on denim by the flat needle method, which was used as the inductance of the sensor coil, and circular tin wire coil was used as the reading coil, which was connected to the ZND impedance analyzer to measure the energy loss in S_{11} mode.

Characterization of Conductive Fabric. The square resistance of the conductive fabric was measured by a four-probe resistance tester (RTS-8). The phase identification of the Ag electrodes was performed by an X-ray diffractometer (X'Pert PRO, PANalytical). The morphology and structure of the prepared materials were examined by scanning electron microscopy (SEM, Hitachi SU-70). The whiteness of the conductive fabric was measured by a whiteness meter (WSB-L).

Characterization of Sensor Response. The mechanical properties and electricity response of the corresponding pressure sensor were measured through a compression test of composites using a micro force tension meter (Instron 5565A) with a load-cell capacity of 100 N. The capacitance of the pressure sensor was measured by an LCR meter (TH8090, Changzhou, China).

Informed Consent. The volunteers (Liyun Ma and Ronghui Wu) agreed to all tests and the picture in the manuscript with informed consent.

■ ASSOCIATED CONTENT

Supporting Information

The Supporting Information is available free of charge on the ACS Publications website at DOI: 10.1021/acsami.9b10928.

Optical images for color- and pattern-reserved conductive fabrics by mask-assisted transferring method. Schema of the strategy for the fabrication of pressure sensor electrode arrays. Electric response when the pressure sensor was under torsion. Pressure mapping by the textile-based pressure-sensing array. Mobile signal display for human motion detected by a pressure-senor-embedded intelligent garment. Cloud servers for human motion information storage by a pressure-senor-embedded intelligent garment. Real-time detection of human coughing detected by a pressure sensor (PDF)

Video S1. Electrical resistance response when the conductive fabric was under mechanical bending (MOV)

Video S2. Real-time detection of human motion when the volunteer wore the intelligent garment with an embedded pressure sensor (MOV)

■ AUTHOR INFORMATION

Corresponding Authors

*E-mail: wdyu@dhu.edu.cn (W.Y.).
*E-mail: wxguo@xmu.edu.cn (W.G.).
*E-mail: phyliuxy@nus.edu.sg (X.Y.L.).

ORCID

Wenxi Guo: 0000-0002-0791-9023
Xiang Yang Liu: 0000-0002-5280-5578

Author Contributions

All authors have given approval to the final version of the manuscript.

Notes

The authors declare no competing financial interest.

■ ACKNOWLEDGMENTS

This work was financially supported by NUS AcRF Tier 1 (R-144-000-367-112), the "111" project (B16029), the National Nature Science Foundation of China (nos. U1405226, 51502253, 21503175, and 21705135), the Shenzhen Basic

DOI: 10.1021/acsami.9b10928
ACS Appl. Mater. Interfaces 2019, 11, 33336−33346

Research Program (no. JCYJ20180306173007696), the Doctoral Fund of the Ministry of Education (20130121110018), the Natural Science Foundation of Fujian Province (grant no. 2017J01104), the Fundamental Research Funds for the Central Universities of China (grant nos. 20720160127 and 20720180013), and the National Key R&D Program of China (2016YFC0802802). We also acknowledge the technical support from Shengshi Guo, Rui Yu, Hao Wang, Li-kun Yang, and Yun Yang.

REFERENCES

(1) Ge, J.; Sun, L.; Zhang, F. R.; Zhang, Y.; Shi, L. A.; Zhao, H. Y.; Zhu, H. W.; Jiang, H. L.; Yu, S. H. A Stretchable Electronic Fabric Artificial Skin with Pressure, Lateral Strain, and Flexion Sensitive Properties. *Adv. Mater.* **2016**, *28* (4), 722−728.

(2) Lee, J.; Kwon, H.; Seo, J.; Shin, S.; Koo, J. H.; Pang, C.; Son, S.; Kim, J. H.; Jang, Y. H.; Kim, D. E.; Lee, T. Conductive Fiber Based Ultrasensitive Textile Pressure Sensor for Wearable Electronics. *Adv. Mater.* **2015**, *27* (15), 2433−2439.

(3) Hu, L.; Pasta, M.; La Mantia, F. L.; Cui, L.; Jeong, S.; Deshazer, H. D.; Choi, J. W.; Han, S. M.; Cui, Y. Stretchable, porous, and conductive energy textiles. *Nano Lett.* **2010**, *10* (2), 708−714.

(4) Zeng, W.; Tao, X.-M.; Chen, S.; Shang, S.; Chan, H. L. W.; Choy, S. H. Highly durable all-fiber nanogenerator for mechanical energy harvesting. *Energy Environ. Sci.* **2013**, *6* (9), 2631−2638.

(5) Li, X.; Qian, K.; He, Y.-B.; Liu, C.; An, D.; Li, Y.; Zhou, D.; Lin, Z.; Li, B.; Yang, Q.-H.; Kang, F. A dual-functional gel-polymer electrolyte for lithium ion batteries with superior rate and safety performances. *J. Mater. Chem. A* **2017**, *5* (35), 18888−18895.

(6) Chang, H. C.; Liu, C. L.; Chen, W. C. Flexible Nonvolatile Transistor Memory Devices Based on One Dimensional Electrospun P3HT:Au Hybrid Nanofibers. *Adv. Funct. Mater.* **2013**, *23* (39), 4960−4968.

(7) Paul, D. L.; Giddens, H.; Paterson, M. G.; Hilton, G. S.; McGeehan, J. P. Impact of Body and Clothing on a Wearable Textile Dual Band Antenna at Digital Television and Wireless Communications Bands. *IEEE Trans. Antennas Propag.* **2013**, *61* (4), 2188−2194.

(8) Zeng, W.; Shu, L.; Li, Q.; Chen, S.; Wang, F.; Tao, X. M. Fiber-based wearable electronics: a review of materials, fabrication, devices, and applications. *Adv. Mater.* **2014**, *26* (31), 5310−5336.

(9) Wang, Q.; Jian, M. Q.; Wang, C. Y.; Zhang, Y. Y. Carbonized Silk Nanofiber Membrane for Transparent and Sensitive Electronic Skin. *Adv. Funct. Mater.* **2017**, *27* (9), 1605657.

(10) Liu, M. M.; Pu, X.; Jiang, C. Y.; Liu, T.; Huang, X.; Chen, L. B.; Du, C. H.; Sun, J. M.; Hu, W. G.; Wang, Z. L. Large-Area All-Textile Pressure Sensors for Monitoring Human Motion and Physiological Signals. *Adv. Mater.* **2017**, *29* (41), 1703700.

(11) Wang, R.; Jiang, N.; Su, J.; Yin, Q.; Zhang, Y.; Liu, Z.; Lin, H.; Moura, F. A.; Yuan, N.; Roth, S.; Rome, R. S.; Ovalle-Robles, R.; Inoue, K.; Yin, S.; Fang, S.; Wang, W.; Ding, J.; Shi, L.; Baughman, R. H.; Liu, Z. A Bi-Sheath Fiber Sensor for Giant Tensile and Torsional Displacements. *Adv. Funct. Mater.* **2017**, *27* (35), 1702134.

(12) Atalay, O.; Atalay, A.; Gafford, J.; Walsh, C. A Highly Sensitive Capacitive-Based Soft Pressure Sensor Based on a Conductive Fabric and a Microporous Dielectric Layer. *Advanced Materials Technologies* **2018**, *3*, 1700237.

(13) Li, J. F.; Xu, B. G. Novel highly sensitive and wearable pressure sensors from conductive three-dimensional fabric structures. *Smart Mater. Struct.* **2015**, *24* (12), 125022.

(14) Pu, X.; Li, L.; Liu, M.; Jiang, C.; Du, C.; Zhao, Z.; Hu, W.; Wang, Z. L. Wearable Self-Charging Power Textile Based on Flexible Yarn Supercapacitors and Fabric Nanogenerators. *Adv. Mater.* **2016**, *28* (1), 98−105.

(15) Paosangthong, W.; Torah, R.; Beeby, S. Recent progress on textile-based triboelectric nanogenerators. *Nano Energy* **2019**, *55*, 401−423.

(16) Guo, Y.; Zhang, X.-S.; Wang, Y.; Gong, W.; Zhang, Q.; Wang, H.; Brugger, J. All-fiber hybrid piezoelectric-enhanced triboelectric nanogenerator for wearable gesture monitoring. *Nano Energy* **2018**, *48*, 152−160.

(17) Eaton, W. P.; Smith, J. H. Micromachined pressure sensors: Review and recent developments. *Smart Mater. Struct.* **1997**, *6* (5), 530−539.

(18) Wang, Z.; Huang, Y.; Sun, J.; Huang, Y.; Hu, H.; Jiang, R.; Gai, W.; Li, G.; Zhi, C. Polyurethane/Cotton/Carbon Nanotubes Core-Spun Yarn as High Reliability Stretchable Strain Sensor for Human Motion Detection. *ACS Appl. Mater. Interfaces* **2016**, *8* (37), 24837−24843.

(19) Wang, C. Y.; Li, X.; Gao, E. L.; Jian, M. Q.; Xia, K. L.; Wang, Q.; Xu, Z. P.; Ren, T. L.; Zhang, Y. Y. Carbonized Silk Fabric for Ultrastretchable, Highly Sensitive, and Wearable Strain Sensors. *Adv. Mater.* **2016**, *28* (31), 6640−6648.

(20) Zhang, M. C.; Wang, C. Y.; Wang, H. M.; Jian, M. Q.; Hao, X. Y.; Zhang, Y. Y. Carbonized Cotton Fabric for High-Performance Wearable Strain Sensors. *Adv. Funct. Mater.* **2017**, *27*, 1604795.

(21) Gong, W.; Hou, C. Y.; Zhou, J.; Guo, Y. B.; Zhang, W.; Li, Y. G.; Zhang, Q. H.; Wang, H. Z. Continuous and scalable manufacture of amphibious energy yarns and textiles. *Nat. Commun.* **2019**, *10* (1), 868.

(22) Yin, B.; Wen, Y.; Hong, T.; Xie, Z.; Yuan, G.; Ji, Q.; Jia, H. Highly Stretchable, Ultrasensitive, and Wearable Strain Sensors Based on Facilely Prepared Reduced Graphene Oxide Woven Fabrics in an Ethanol Flame. *ACS Appl. Mater. Interfaces* **2017**, *9* (37), 32054−32064.

(23) He, S.; Xin, B.; Chen, Z.; Liu, Y. Flexible and highly conductive Ag/G-coated cotton fabric based on graphene dipping and silver magnetron sputtering. *Cellulose* **2018**, *25* (6), 3691−3701.

(24) Cai, G.; Xu, Z.; Yang, M.; Tang, B.; Wang, X. Functionalization of cotton fabrics through thermal reduction of graphene oxide. *Appl. Surf. Sci.* **2017**, *393*, 441−448.

(25) Qu, L.; Tian, M.; Hu, X.; Wang, Y.; Zhu, S.; Guo, X.; Han, G.; Zhang, X.; Sun, K.; Tang, X. Functionalization of cotton fabric at low graphene nanoplate content for ultrastrong ultraviolet blocking. *Carbon* **2014**, *80*, 565−574.

(26) Du, Z. Q.; Li, M.; Wu, Y. X.; He, L. G. Analysis of spherical compression performance of warp-knitted spacer fabrics. *J. Ind. Text.* **2017**, *46* (6), 1362−1378.

(27) Hasani, H.; Ajeli, S.; Hessami, R.; Zadhoush, A. Investigation into energy absorption capacity of composites reinforced by three-dimensional-weft knitted fabrics. *J. Ind. Text.* **2014**, *43* (4), 536−548.

(28) Liu, Y.; Hu, H. Compression property and air permeability of weft knitted spacer fabrics. *J. Text. Inst.* **2011**, *102* (4), 366−372.

(29) Tan, Q. L.; Lv, W.; Ji, Y. H.; Song, R. J.; Lu, F.; Dong, H. L.; Zhang, W. D.; Xiong, J. J. A LC wireless passive temperature-pressure-humidity (TPH) sensor integrated on LTCC ceramic for harsh monitoring. *Sens. Actuators, B* **2018**, *270*, 433−442.

(30) Boutry, C. M.; Beker, L.; Kaizawa, Y.; Vassos, C.; Tran, H.; Hinckley, A. C.; Pfattner, R.; Niu, S. M.; Li, J. H.; Claverie, J.; Wang, Z.; Chang, J.; Fox, P. M.; Bao, Z. N. Biodegradable and flexible arterial-pulse sensor for the wireless monitoring of blood flow. *Nat. Biomed Eng.* **2019**, *3* (1), 47−57.

(31) Nie, B.; Huang, R.; Yao, T.; Zhang, Y.; Miao, Y.; Liu, C.; Liu, J.; Chen, X. Textile Based Wireless Pressure Sensor Array for Human Interactive Sensing. *Adv. Funct. Mater.* **2019**, *29*, 1808786.

(32) He, S.; Xin, B. J.; Chen, Z. M.; Liu, Y. Flexible and highly conductive Ag/G-coated cotton fabric based on graphene dipping and silver magnetron sputtering. *Cellulose* **2018**, *25* (6), 3691−3701.

(33) Yu, W; Chu, C. *Textile Physics*; Donghua University Press, 2009.

(34) Zhang, F.; Li, W.; Xu, Z.; Ye, M.; Guo, W.; Xu, H.; Liu, X. Transparent conducting oxide- and Pt-free flexible photo-rechargeable electric energy storage systems. *RSC Adv.* **2017**, *7* (83), 52988−52994.

(35) Chen, B.; Xing, Y.; Yu, W.; Liu, H. Wool keratin and silk sericin composite films reinforced by molecular network reconstruction. *J. Mater. Sci.* **2018**, *53* (7), 5418−5428.

DOI: 10.1021/acsami.9b10928
ACS Appl. Mater. Interfaces 2019, 11, 33336−33346

(36) Harada, S.; Honda, W.; Arie, T.; Akita, S.; Takei, K. Fully printed, highly sensitive multifunctional artificial electronic whisker arrays integrated with strain and temperature sensors. *ACS Nano* **2014**, *8* (4), 3921−3927.
(37) Hong, S. Y.; Lee, Y. H.; Park, H.; Jin, S. W.; Jeong, Y. R.; Yun, J.; You, I.; Zi, G.; Ha, J. S. Stretchable Active Matrix Temperature Sensor Array of Polyaniline Nanofibers for Electronic Skin. *Adv. Mater.* **2016**, *28* (5), 930−935.

DOI: 10.1021/acsami.9b10928
ACS Appl. Mater. Interfaces 2019, 11, 33336−33346